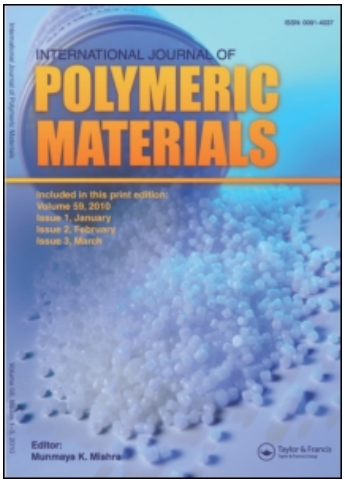

International Journal of Polymeric Materials
Publication details, including instructions for authors and subscription information:
http://www.informaworld.com/smpp/title~content=t713647664

Nanosilica-Reinforced Polypropylene Composites: Microstructural Analysis and Crystallization Behavior

M. S. Sreekala[a]; B. Lehmann[a]; K. Friedrich[a]; M. Z. Rong[b]
[a] Institute for Composite Materials (IVW GmbH), University of Kaiserslautern, Kaiserslautern, Germany [b] Materials Science Institute, Zhongshan University, Guangzhou, People's Republic of China

To cite this Article Sreekala, M. S. , Lehmann, B. , Friedrich, K. and Rong, M. Z.(2006) 'Nanosilica-Reinforced Polypropylene Composites: Microstructural Analysis and Crystallization Behavior', International Journal of Polymeric Materials, 55: 8, 577 — 594
To link to this Article: DOI: 10.1080/00914030500236874
URL: http://dx.doi.org/10.1080/00914030500236874

International Journal of Polymeric Materials, 55:577–594, 2006

ISSN: 0091-4037 print/1563-5333 online
DOI: 10.1080/00914030500236874

Taylor & Francis
Taylor & Francis Group

Nanosilica-Reinforced Polypropylene Composites: Microstructural Analysis and Crystallization Behavior

M. S. Sreekala
B. Lehmann
K. Friedrich
Institute for Composite Materials (IVW GmbH), University of Kaiserslautern, Kaiserslautern, Germany

M. Z. Rong
Materials Science Institute, Zhongshan University, Guangzhou, People's Republic of China

Polypropylene (PP) was reinforced with polystyrene-grafted nanosilica particles. A detailed study on the microstructure of untreated and treated nano-SiO_2-particle–reinforced polypropylene composites has been made by using Atomic Force Microscopy (AFM) and Transmission Electron Microscopy (TEM). The observations were correlated with the properties of the composites. Characterization of the microstructure of the nanocomposites led to a better understanding of the mechanisms of improvement in properties upon modified nanosilica reinforcement. Dispersion characteristics of the nanoparticles and the extent of agglomerate formation became clear from the AFM and TEM examinations. In order to analyze the nanomechanical properties of the composite, microscratching and nanoindentation studies were carried out using AFM. The effect of particle reinforcement on the crystallization behavior of the composites has been studied. Crystallization kinetics has been analyzed by Differential Scanning Calorimetric (DSC) measurements. The nature of nucleation and crystal growth process has been investigated by optical microscopy. The dynamic mechanical properties, microhardness, and the wear properties of the nanocomposites were examined as a function of filler content.

Received 2 June 2005; in final form 15 June 2005.

One author (M. S. S.) wishes to thank the Alexander von Humboldt Foundation, Bonn, Germany for the research fellowship at Institute for Composite Materials (IVW GmbH), University of Kaiserslautern. Thanks also to Dr. Harald Fuge, Biology Department, University of Kaiserslautern for his support in Transmission Electron Microscopic studies.

Address correspondence to K. Friedrich, Institute for Composite Materials (IVW GmbH), University of Kaiserslautern, Erwin-Schrödinger-Strasse, Bldg. 58, 67663 Kaiserslautern, Germany. E-mail: friedrich@ivw.uni-kl.de

Keywords: nanocomposites, polypropylene, crystallization, Atomic Force Microscopy, Transmission Electron Microscopy, Differential Scanning Calorimetry, optical microscopy

INTRODUCTION

Now-a-days polymer nanocomposites in general have attracted a significant research interest because they can lead to a wide applicability due to their ability to attain exceptional properties as a result of their nanostructure. They are identified as having excellent strength, optical, and thermal properties [1]. The existing processing techniques for nanocomposites such as sol-gel process, intercalation polymerization in layered silicate nanocomposites and so on are known to have various limitations because they require complex polymerization procedures and special solvents, show difficulty in controlling the reaction, and have limited commercial applicability. While following the conventional processing techniques, the main difficulty in achieving optimum properties of polymer nanocomposites often are due to the strong tendency of nanoparticles to agglomerate. This is hard to control by the limited shear forces during the mixing procedure.

In the present work, a conventional compounding technique, using a single screw extruder is followed for the preparation of nano-SiO_2-particle reinforced Polypropylene (PP) composites. The possibility of eliminating dispersion problems in the nanocomposites, thereby improving their strength and toughness, was studied. Surface modification of nanoparticles has been done through irradiation grafting of the particles with polystyrene monomer, which is a simple, low cost, and easily controlled. The microstructure of the composite has been studied in detail. It has been reported that nanoparticle reinforcement in polymers affects the crystallization behavior of the system [2]. Kinetic analysis of the crystallization process has been done following the general theory developed by Avrami [3]. The nature and time dependence of the nucleation process has again been confirmed by optical microscopic studies. Dynamic mechanical properties of the composites were investigated as a function of temperature. The ultramicrohardness and wear properties of the composites were analyzed.

MATERIALS AND EXPERIMENTAL

An isotactic PP homopolymer having melt flow index of 6.7 g/10 min and nanoparticles of SiO_2 having diameter of 7 nm were used in the study. Styrene monomer has been grafted onto the particles by ^{60}Co

γ-ray irradiation at a dose rate of 1 Mrad/h in air. The nanocomposites were prepared by melt mixing in a single screw extruder at 200°C and 25 rpm. The details of irradiation technique and sample preparation were reported elsewhere [4]. Compression-molded specimens having nanosilica volume percentage of 0.39, 0.65, 1.96, 3.31, and 4.68% were used for the analysis.

Atomic Force Microscopy

Atomic force microscope from Digital Instruments (Nanoscope III) was used to study the structural characterization of the nanocomposites. AFM images of the nanocomposite surfaces were taken using tapping mode. Nanoindentation tests and microscratching were done using scanning probe microscope (SPM) lithography mode of the AFM. A detailed description of the instrumentation and various modes of AFM imaging were reported earlier from this institute [5].

Transmission Electron Microscopy

Ultra-thin sections of the nanocomposites were cut at room temperature using an ultramicrotome (LKB Ultrotome III) equipped with a diamond knife at a cutting speed of 20 mm/s with a thermal feed of 50–60 nm. TEM images were taken on a Zeiss EM 10A transmission electron microscope using an accelerating voltage of 80 keV.

Microhardness Measurements

Dynamic microhardness of the nanocomposites has been done on a dynamic ultramicrohardness tester from DUH—202 Shimadzu Corporation, Japan. A load of 500 mN was used to make microindentations. Ten measurements were made and average value is reported.

Friction and Wear Measurements

Friction coefficient and the specific wear rate of the nanocomposites were determined from sliding wear tests on a pin-on-ring apparatus with carbon steel ring as the counterpart. A pressure of 1 MPa and a velocity of 1 m/s were used for a duration of 10 h.

Scanning Electron Microscopy (SEM)

SEM photographs were taken on a JEOL JSM—5400 scanning microscope. A sputtering device from Balzers SCD 050 sputter coater was

used to make a conductive coating on the sample surface. An accelerating voltage of 20 kV was used for the investigation.

Dynamic Mechanical Analysis

A dynamic mechanical thermal analyzer from GABO Qualimeter was employed for dynamic mechanical properties evaluation of the composites. Bending dynamic force has been applied at a frequency of 10 Hz and at a heating rate of 1°C/min for a temperature range of −140 to 150°C.

Crystallization Studies

Differential Scanning Calorimetry (DSC)

Isothermal and nonisothermal crystallization behavior of the Nanosilica/PP composites were investigated on DSC 30 and DSC 821 apparatus from Mettler Toledo, respectively. Isothermal crystallization of the composites was done by heating the sample from 30°C to 220°C at a heating rate of 25°C/min, holding at 220°C for 2 min, cooling from 220°C to respective temperatures (118, 120, 123, 125, 127, 130, 132°C) at a cooling rate of 50°C/min, holding at the temperature until complete recrystallization and no further change in enthalpy occurs. Dynamic crystallization behavior has been examined by heating the sample from 30°C to 220°C, cooling from 220°C to 30°C, reheating from 30°C to 220°C, again cooling from 220°C to 30°C at a heating or cooling rate of 20°C/min. All the measurements were conducted in nitrogen atmosphere. The degree of crystallinity of the nanocomposites was calculated from the ratio of the enthalpy of fusion of the composites and the enthalpy of fusion of the perfectly crystalline isotactic PP (190 J/g). Kinetics of isothermal crystallization was analyzed by using the Avrami relationship [6]

$$\ln\{-\ln[1 - X(t, T)]\} = \ln k(T) + n \ln t \quad (1)$$

where X(t, T) is the relative crystallinity at time t and at isothermal crystallization temperature T, n is the Avrami exponent that explains the dimensionality of the spherulite growth process and the kinetic order of nucleation, and k is the crystallization rate coefficient, which is a parameter of crystallization growth rate and is related to the nucleation type, crystal growth geometry, and crystallization temperature. The values of n and k were calculated from the slope and y intercept of the Avrami plot of $\ln[-\ln(1 - X)]$ versus $\ln t$.

Hot-Stage Optical Microscopy

Hot-stage polarized light microscopic measurements on the morphology of sperulitic growth and crystallization were done on a Linkam TMS 91 hot-stage and a Leitz Diaplan microscope. Thin specimens were cut from compression-molded specimens using a microtome and were isothermally crystallized on the microscope stage at different temperatures (118, 127, and 132°C).

RESULTS AND DISCUSSION

Microstructure by AFM and TEM

The main problem encountered during the preparation of polymer nanocomposites was the formation of clusters, agglomerates, and aggregation of particles within the matrix, which caused a decline in the end properties. To alleviate these problems, polymer grafting onto the nanoparticles was employed before incorporating into the matrix polymer. It was reported earlier that incorporation of the polymer grafted nanosilica into PP matrix considerably improved the toughness and stiffness of the composite [4]. Polymer grafting will improve the microstructure of the system. Modified particles in the matrix will lead to good dispersion, entanglement of the grafting and matrix polymers, and higher rigidity of the agglomerates. The nature and dispersion of the grafted nanoparticles in the PP matrix at various filler content was evident from the AFM and TEM images (Figures 1a, b and 2a–d).

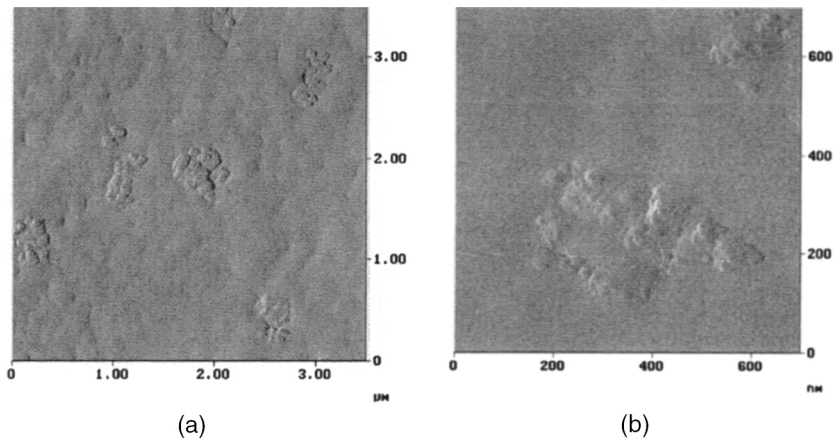

(a) (b)

FIGURE 1 AFM images of the SiO_2-g-PS/PP nanocomposites (SiO_2 vol% = 1.96).

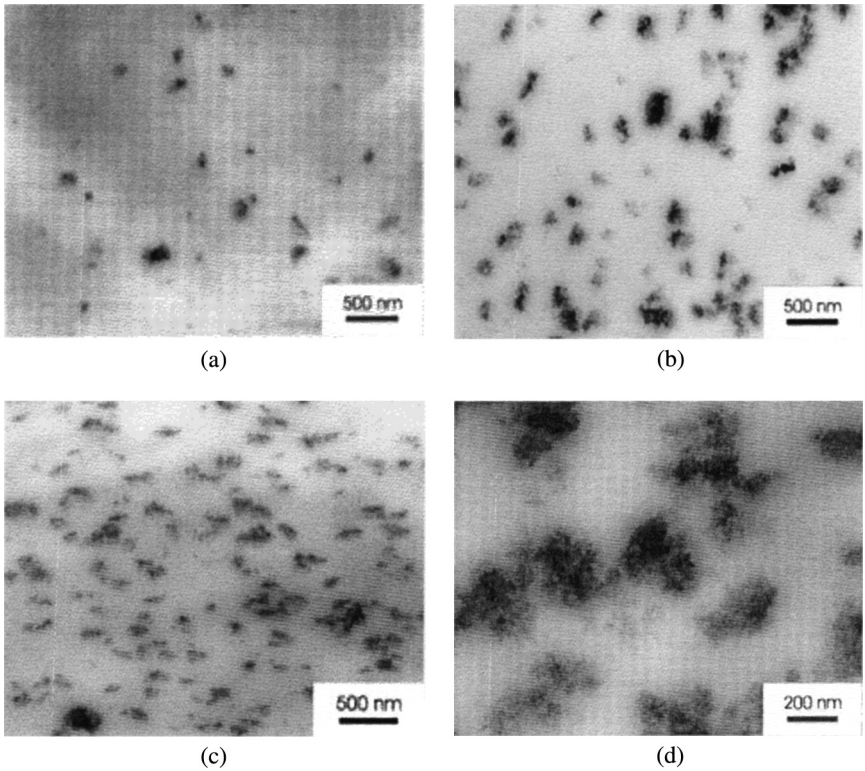

FIGURE 2 TEM of the SiO_2-g-PS/PP nanocomposites (a) SiO_2 vol% = 0.39, (b) SiO_2 vol% = 1.96, (c) and (d) SiO_2 vol% = 4.68.

A uniform dispersion of the agglomerates consisting of a larger amount of nanoparticles was observed. It was found that the grafting polymer had penetrated into the agglomerate network making it more rigid and providing better stress transfer between the agglomerate and the surrounding matrix (Figures 1b and 2d) [4]. Average agglomerate size was found to be 300 nm. The structure of the agglomerates revealed the penetration of the matrix polymer.

Microscratching and Nanoindentation

Figure 3 shows a microscratch made on the nanosilica-filled PP composite by SPM lithography. The harder silica particles were found to be more resistant to deformation upon microscratch and nanoindentation. The scratch depth in matrix region is 77 and in agglomerate is

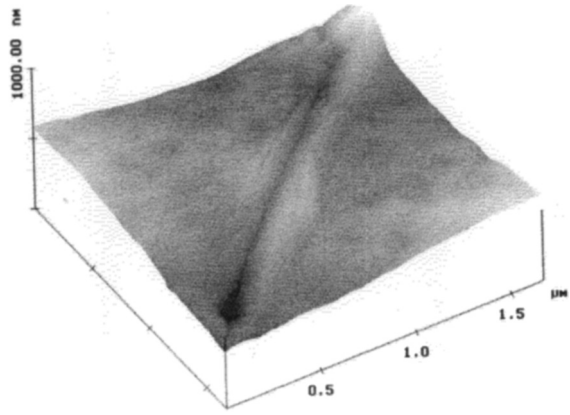

FIGURE 3 AFM image of a microscratch on SiO_2-g-PS/PP composite.

75 nm. Petrovicova et al. [7] reported the microscratching studies on nylon/nanosilica composites. They observed higher scratch resistances with nanoparticle reinforcement due to the higher crystallinity.

Equidistant nanoscale indentations ($\Delta = 0{,}5\,\mu m$) were made on the PP/PS-g-SiO_2 nanocomposite using the pyramidal-shaped indenter. Applied peak forces of 50 μN led to indentation depths of about 160 nm. The neat matrix material was examined as a reference to compare the modulus and hardness values with those of the nanocomposite (Figures 4 and 5). For performing indentations into the nanocomposite, a nanoparticle agglomerate was first detected. The series of indentations was then set along a line, started within the matrix,

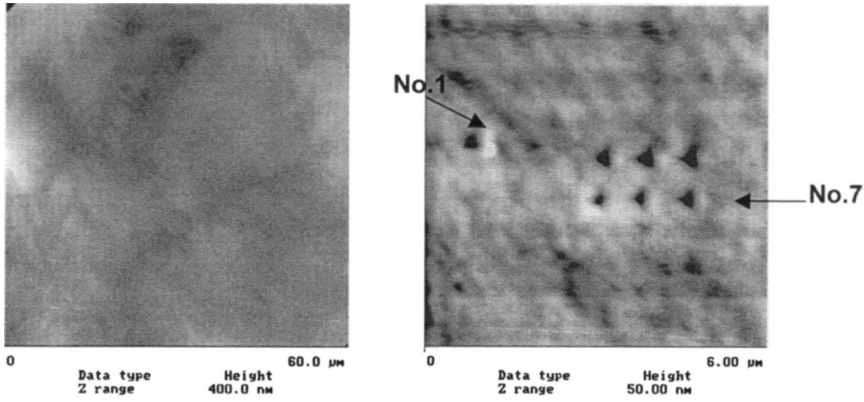

FIGURE 4 Atomic force microscope surface scans of Left: neat PP, Right: PP with nano-indentations performed by the TriboScope system.

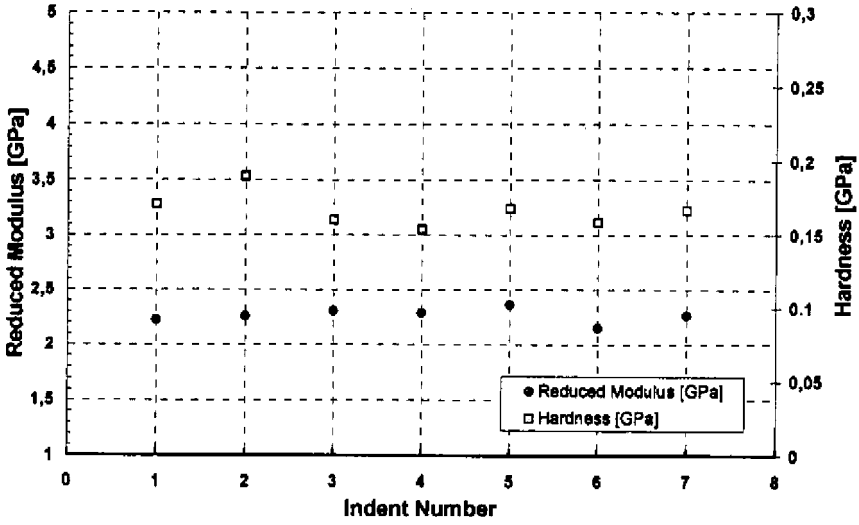

FIGURE 5 Reduced modulus and hardness for neat PP. Indentations are numbered starting at the left upper corner to the right corner in Figure 4, right hand side.

crossed the matrix/particle interface and the agglomerate's center, and finally ended in the matrix again.

It is clearly shown in Figure 6 that significant differences in modulus and hardness in the vicinity of the agglomerates occur. The values increase at the particle/matrix interface reaching notably higher values inside the agglomerate. Matrix modulus and hardness here correspond directly to the values measured for the neat PP (Figure 5). Increased values were detected within the nanoparticle agglomerate.

The reduced modulus is defined by the equation $E_r = S(\sqrt{\pi}/(2\sqrt{A}))$ where S is the unloading stiffiness, calculated from the unloading force/displacement curve, and A is the projected contact area. The reduced modules is related to the modulus of elasticity E through the equation $1/E_r = (1-\nu_1^2)/E_1 + (1-\nu_2^2)/E_2$ were ν_1, ν_2 represent the Poisson's ratio of the diamond tip and the indented material, respectively. The variation of the loading speed and holding time could be used to consider the viscoelasticity of the polymer.

Dynamic Ultramicrohardness

Ultra microhardness showed irregular variation with filler content (Table 1). Upon nanosilica reinforcement, it has been observed that

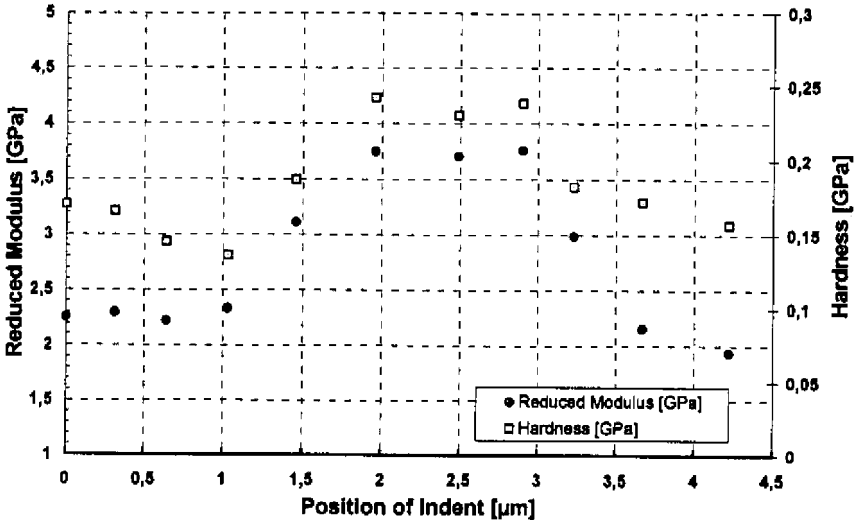

FIGURE 6 Reduced modulus and hardness for PP/PS-g-SiO_2 nanocomposite.

the microhardness values initially decrease. However considerable increase has been observed upon higher filler content of 4.68 vol%. It has been already reported that the microhardness of crystalline polymers is dependent on the specific morphology of the material [8]. The micro-indendation hardness depends on the local molecular and supermolecular deformations at the surface of the polymer. The degree of crystallinity and the dispersion of the nanosilica in PP matrix affect the variation in ultramicrohardness of the

TABLE 1 Dynamic Ultramicrohardness, Wear Rate and Friction Coefficient Values of PP/PS-g-SiO_2 Nanocomposite

	Ultramicrohardness HU (MPa)		Specific wear rate (Ws) (10^{-5} mm^3/Nm)		Friction Coefficient (μ)	
Filler content volume (%)	HU	[Standard deviation]	Ws	[Standard deviation]	μ	[Standard deviation]
Neat PP	121	6.77	0.17	0.063	8.53	3.44
0.39	113	5.59	5.74	0.45	8.8	1.53
0.65	111	3.34	3.95	0.39	7.29	3.51
1.96	112	4.41	4.68	0.97	9.31	0.86
3.31	117	5.69	3.93	0.53	8.03	4.24
4.68	130	10.69	—	—	—	—

composites. The crystallinity decreased upon the addition of small amount of nanosilica; however, it shows considerable increase at higher nanosilica content as discussed later. The deformation behavior of the agglomerates during microindentation affects the hardness value. At lower silica loading, the matrix deformation is easier due to the absence of agglomerates in the immediate vicinity. At higher silica loading more closely packed arrangement of rigid agglomerates is observed, which marginally increases the microhardness of the system (Figure 4). The harder silica particles were more resistant to deformation upon nanoindentation. Also the spherulite morphology of the composites and the neat sample developed under the preparation conditions will affect the microhardness values. The large spherulite size expected in gum sample gives higher microhardness values. At higher filler content, the number of spherulites is higher, which again explains the increase in microhardness.

Wear Rate and Friction Coefficient

The specific wear rate value shows considerable enhancement upon nanosilica reinforcement (Table 1). It is reported that the presence of agglomerates in epoxy nanocomposites facilitates the disintegration of the material upon wearing [9]. However, a small decrease in wear rate is observed with increase in filler content within the reinforced composites. At lower filler content, the lower number of agglomerates surrounded by the matrix material will be prone to easy disintegration. At higher filler content, the adjacent silica agglomerates will somewhat prevent the disintegration. This is more evident from the SEM pictures of the worn surfaces (Figure 7a, b, and c). More adhesive wear is observed at 0.65 vol% nanosilica-filled composite. This is clear from the presence of considerable amount of worn out matrix material. In the neat PP and 3.31 vol% nanosilica-filled sample, more abrasive-type wear is observed, which is evident from the nature of the worn surface. The friction coefficient shows irregular trend with filler content; it is dependent on the surface topography and the nature of the filler dispersion in the matrix.

Dynamic Mechanical Properties

Storage modulus, mechanical damping, and loss modulus of the neat PP and filled nanocomposites are given in Figure 8 (a, b,

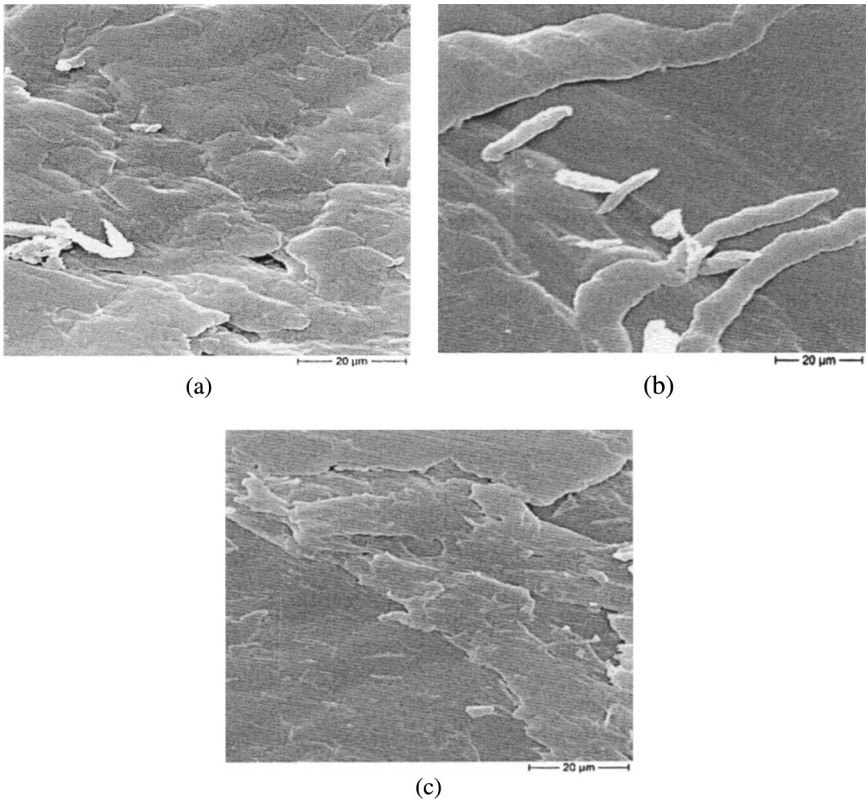

(a) (b)

(c)

FIGURE 7 SEM of worn surfaces of (a) neat PP, (b) PP/PS-g-SiO_2 nanocomposite having 0.65 vol% of SiO_2, (c) PP/PS-g-SiO_2 nanocomposite having 3.31 vol% of SiO_2.

and c). The modulus of the material increased upon nanosilica reinforcement as observed at the high temperature region. This is due to the presence of elastic filler and their better interaction with the matrix PP. The mechanical damping decreases upon nanosilica reinforcement. A shift in the T_g value toward the higher temperature region is observed upon nanosilica reinforcement. T_g value of 7, 18.8, 18.9, and 15.6°C were observed from tan δ measurement for the neat PP and 0.65, 1.96, and 3.31 vol% nanosilica-filled composites, respectively. Lower T_g values, 3.8, 12.7, 15.7, and 12.8°C were observed from loss modulus measurement, respectively, for the same composites.

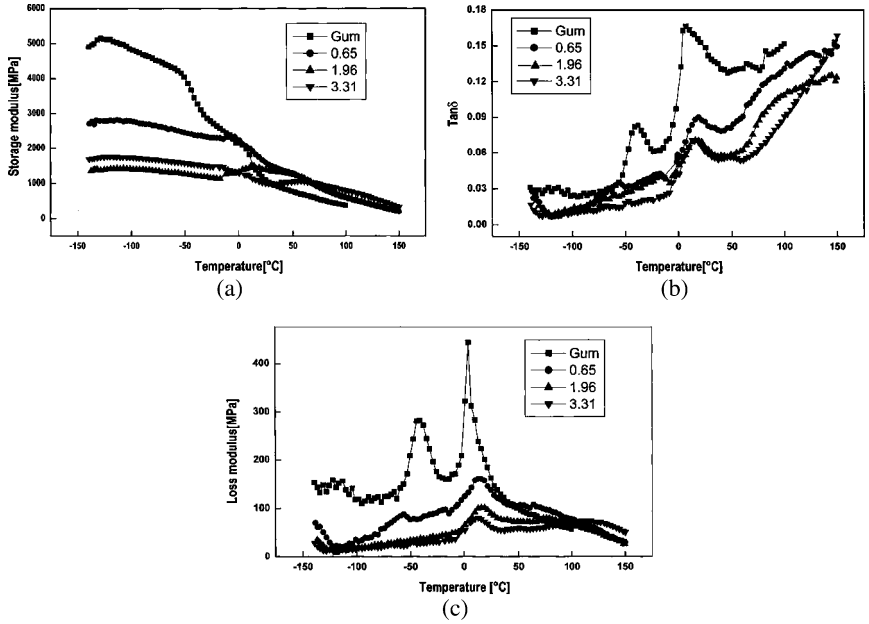

FIGURE 8 (a) Variation in storage modulus of PP/PS-g-SiO_2 nanocomposite. (b) Variation in mechanical damping behavior of PP/PS-g-SiO_2 nanocomposite. (c) Variation in loss modulus of PP/PS-g-SiO_2 nanocomposite.

Crystallization Behavior

The influence of the nanosilica reinforcement upon the crystallization behavior of the PP was analyzed by DSC and optical microscopy. It has already been reported that in clay/PP nanocomposites, the clay particles act as nucleating agent for the matrix PP [10]. It was also found that crystallization influences the morphology and mechanical properties of the nanocomposites. From the dynamic DSC measurements, it has been found that the nanosilica content affects the crystallinity of the system (Figure 9). Crystallinity shows enhancement upon the addition of nanosilica except for a small decrease observed at very low filler content. The onset, endset, and T_C, the crystallization temperature are given in Table 2. Upon nanosilica reinforcement the crystallization rate increases considerably $[1/(T_0 - T_C) = rate]$. The crystallization starts at higher temperature as the filler content increases. Presence of nanoparticels facilitates the crystallization process. Isothermal crystallization kinetics analyzed by the Avrami theory are given in Table 3. The avrami

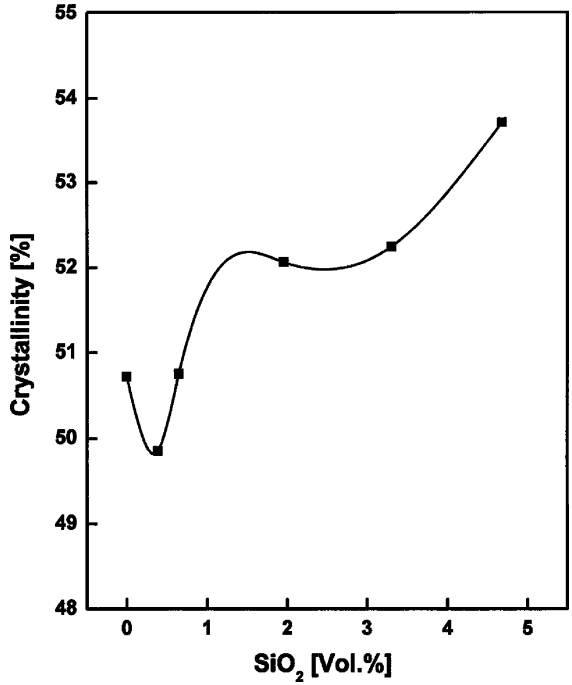

FIGURE 9 Variation in crystallinity of the PP/PS-g-SiO_2 nanocomposite with filler content.

exponent n, and the rate constant ln k show irregular variation with filler content and at different isothermal temperatures. Comparatively higher values of "n" were observed in nanosilica-filled systems. The three-dimensional crystal growth will be influenced by the

TABLE 2 Onset, Endset and Tc for the Dynamic Crystallization of PP/PS-g-SiO_2 Nanocomposite

Filler content volume (%)	Onset temperature T_0 (°C)	Endset temperature (°C)	Tc (°C)
Neat PP	118.05	100.58	113.51
0.39	119.63	108.36	116.33
0.65	120.18	108.40	116.99
1.96	120.62	105.63	116.86
3.31	120.89	109.37	118.10
4.68	121.24	105.75	117.53

TABLE 3 Avrami Exponent, n and Rate Constant, ln k for the Isothermal Crystallization of PP/PS-g-SiO_2 Nanocomposite

Filler content volume (%)	Isothermal temperature (°C)	Avrami exponent, n	Rate constant, ln k
Neat PP	118	3.17	−14.30
	120	1.86	−7.06
	123	0.73	−3.44
	125	1.71	−8.00
	127	1.31	−6.80
	130	1.42	−9.38
	132	0.87	−9.48
0.39	118	1.88	−7.83
	120	1.75	−7.27
	123	1.44	−5.84
	125	1.17	−5.02
	127	1.45	−7.08
	130	2.91	−15.58
	132	1.45	−10.35
1.96	118	1.72	−6.95
	120	2.00	−8.48
	123	1.12	−5.43
	125	0.92	−10.93
	127	0.89	−5.31
	130	1.01	−5.76
	132	1.37	−7.23
4.68	118	2.05	−8.36
	120	1.85	−7.73
	123	2.41	−11.04
	125	1.14	−4.75
	127	1.18	−5.47
	130	2.30	−11.78
	132	1.58	−9.58

presence of nanosilica agglomerates. This is dependent on whether the particles are present in the vicinity of spherulitic growth. Hence, an irregular trend is expected in these composites. In most cases the values are in between 1 and 3, which explains the random nucleation behavior. Irregular trend observed in the rate constant also explains the scattered rates of crystallization process in the nanosilica-filled PP system. The isothermal crystallization thermograms are given in Figure 10 (a, b, c, and d). The curves explain the rapid crystallization process at low temperatures.

The kinetics of crystallization was again confirmed by hot stage optical microscopical analysis of some selected samples. The formation

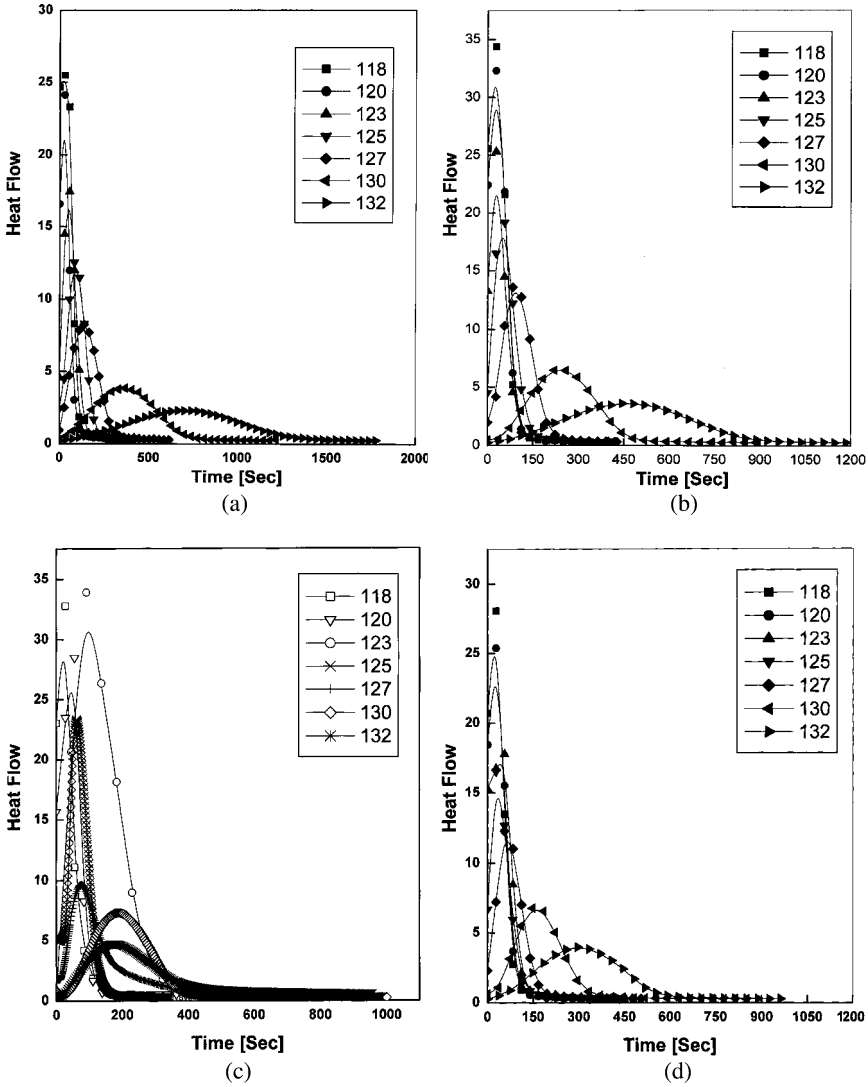

FIGURE 10 Isothermal crystallization thermograms of PP/PS-g-SiO_2 nanocomposite at differnet temperatures. (a) Gum, (b) SiO_2 vol% – 0.39, (c) SiO_2 vol% – 1.96, (d) SiO_2 vol% – 4.68.

of spherulites was observed to be random. The spherulitic growth with time is plotted in Figure 11 (a, b, and c). The rate of spherulitic growth is evident from the increase in the area of spherulites with time.

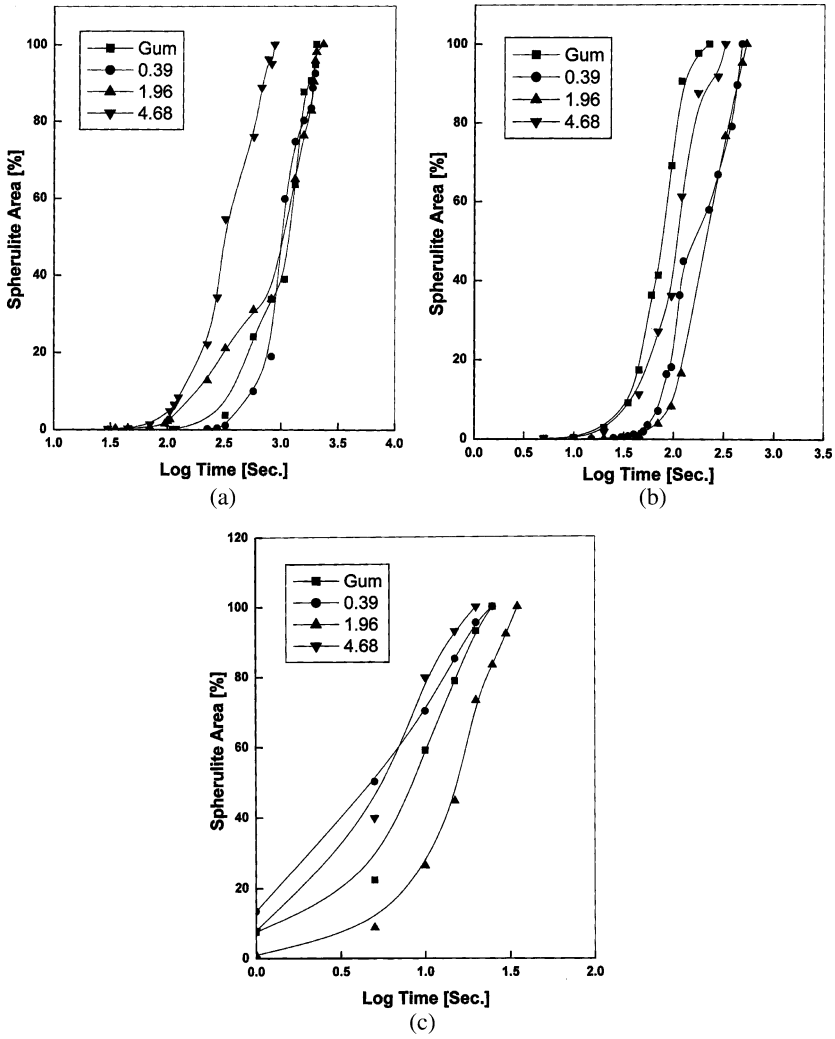

FIGURE 11 Sperulitic area as a function of crystallization time for PP/PS-g-SiO_2 nanocomposite having nanosilica composites. (a) 118°C, (b) 127°C, (c) 132°C.

At higher temperature a rapid increase in the area of spherulites has been found in 4.68 vol% filled composite. From this it can be concluded that the reinforcing nanosilica acts as nucleating agent during crystallization. The differences in the texture of the spherulites upon nanosilica reinforcement is shown in Figure 12.

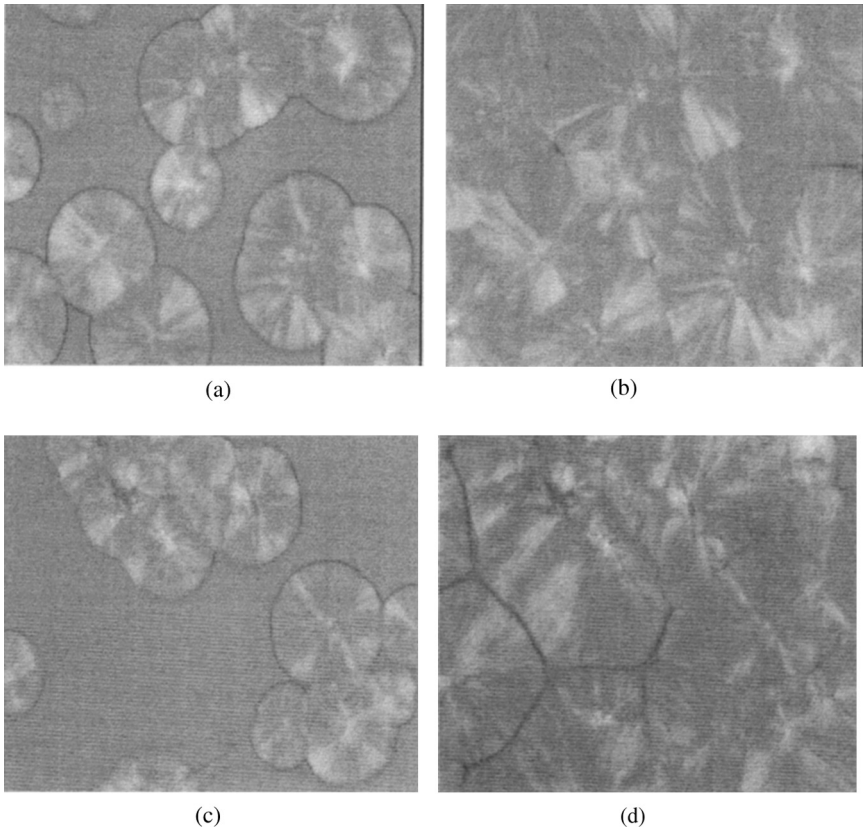

FIGURE 12 Optical micrographs of PP gum (a) after 80 s, (b) after 275 s, and PP/PS-g-SiO_2 nanocomposite having nanosilica vol% 4.68, (c) after 80 s, (d) after 275 s at isothermal temperature of 127°C.

CONCLUSIONS

Microstructure and properties of PP/PS-g-SiO_2 nanocomposites have been analyzed. AFM and TEM micrography well explained the nanoparticle distribution characteristics within the PP matrix. Good interaction of the matrix PP and the grafted polymer made the nanoparticle agglomerate more rigid. This led to better performance of the composites. Microscratching and nanoindentation studies explained the enhanced modulus and hardness of the reinforced systems. However, the dynamic ultramicrohardness showed slight decrease at lower filler content. The presence of nanoparticle agglomerates enhanced the wear rate of the composites. The storage modulus and glass transition

temperature increase upon nanosilica reinforcement. Crystallization studies by DSC and optical microscopy revealed the effect of nanosilica on the spherulitic growth and crystallization kinetics. The degree of crystallinity increased upon nanosilica reinforcement.

REFERENCES

[1] Giannelis, E. P., *Adv. Mater.* **8** (1), 29 (1996).
[2] Ke, Y., Yang, Z., and Zhu, C., *J. Appl. Polym. Sci.* **85**, 2677 (2002).
[3] Bodor, G. (Ed.) (1991). *Structural Investigation of Polymers*, Akademiai Kiado, Budapest.
[4] Rong, M. Z., Zang, M. Q., Zheng, Y. X., Zeng, H. M., Walter, R., and Friedrich, K., *Polymer* **42**, 167 (2001).
[5] Han, Y., Schmitt, S., and Friedrich, K., *Appl. Comp. Mater.* **6**, 1 (1999).
[6] Li, J., Shanks, R. A., and Long, Y., *J. Appl. Polym. Sci.* **82**, 628 (2001).
[7] Petrovicova, E., Knight, R., Schadler, L. S., and Twardowski, T. E., *J. Appl. Polym. Sci.* **78**, 2272 (2000).
[8] Calleja, F. J. B., Boneva, D., Krumove, M., and Fakirov, S., *Macromol. Chem. Phys.* **199**, 2217 (1998).
[9] Rong, M. Z., Zhang, M. Q., Liu, H., Zeng, H., Wetzel, B., and Friedrich, K., *Industrial Lubrication and Tribology* **53**, 72 (2001).
[10] Maiti, P., Nam, P. H., Okamoto, M., Hasegawa, N., and Usuki, A., *Macromolecules* **35**, 2042 (2002).